Tracking for CLAS12

TRACKING GROUP

May 18, 2005

Abstract

We present a conceptual design for a tracking system for CLAS12, an upgraded version of the CLAS detector planned for the Jlab upgrade. In addition to a description of the proposed detectors, we also show a simulation of their expected performance.

1 Constraints and Requirements

Jlab is planning to upgrade its present 6 GeV accelerator to 12 GeV. To take advantage of the new physics opportunities, the Hall B group is designing a new and improved large-acceptance detector, "CLAS12". Because average particle momenta will be higher, the resolution of the tracking system must be better than the current CLAS values; the goal for the fractional momentum resolution is 1% at a track momentum of 5 GeV/c. Likewise, cross-sections for reactions of interest are expected to be small, so the new detector is being designed to operated at a luminosity of 10ˆ35. This higher luminosity goal necessitates the use of a solenoidal magnet to shield the detector from Moller electrons. To reduce interactions between this solenoidal field and a toroidal field and to facilitate construction and installation of new detector elements, the torus has been re-designed. It is more compact than the present torus while providing equivalent bending power. We have designed the tracking detectors with these external constraints: a central solenoid of 5T central field value and a radius available for tracking detectors of 25 cm, a new torus with a different aspect ratio but with the same number of Amp-turns as the present CLAS torus, an expected background rate consistent with a luminosity of 10ˆ35 and a separation between "forward" and "central" regions defined to be at 35 degrees.

2 Design

In this section, we present a design for the forward tracking system consisting of several planes of Silicon strip detectors followed by three "regions" of drift chambers. We also present three alternatives for the central tracking: cathode pad chambers, stereo chamber and a Silicon strip version.

2.1 Forward Drift Chambers

The design of the forward chambers is very similar to the present CLAS chambers. The cell design is hexagonal and the sense wire layers are arranged in 6-layer superlayers as in the present chambers. The major difference is that the cells are approximately half as big as the present chambers allowing efficient tracking at much higher luminosities because the accidental occupancy from particles not associated with the event is much smaller. Table 1 lists the design parameters and Figure fwd-dc-design-drawing shows a cut-view of the layer and superlayer arrangement of the wires. For the purposes of simulating track resolutions we assumed that the position resolution of the individual drift cells would be 200 microns.

	Region 1	**Region 2**	**Region 3**
dist. from target	2.2 m	3.3 m	4.7 m
num. of superlayers	2	2	2
layers/superlayer	6	6	6
wires/layer	144	144	144
cell size	0.8 cm	1.2 cm	1.7 cm
assumed resolution per wire	0.02 cm	0.02 cm	0.02 cm

Table 1:

2.2 Forward Silicon Tracker

The forward Silicon tracker consists of three double-sided Silicon strip detector planes. Each plane is formed from six pieces, each roughly triangular in shape with strips on one plane running parallel to one of the sides of the triangle with readout on the outer-radius side and strips from the other plane being parallel to the other side of the triangle. In this way, the strips cover the entire area of the triangular surface and always run to the "outside" where the readout electronics is located. The strips vary in length, from the longest which is adjacent to its parallel side down to a short strip opposited. See Figure fwd_silicon_tracker_drawing for a layout of the detector and Table 2 for the detector specifications.

2.3 Central Tracking Chambers

There are three options for a central tracker: a cathode pad chamber, a stereo wire chamber or a Silicon strip detector. Each design consists of concentric shells of measurement layers at successively greater radius. The r-phi coordinate is measured by drift time for the two wire chambers or by the Silicon strip coordinate for the Silicon tracker. The r-z coordinate is measured by the charge-weighted pad centroid for the pad chamber, or by a stereo angle projection for

	Region 1	Region 2	Region 3
dist. from target	10 cm	18 cm	26 cm
num. u/v strips	?	?	?
stereo angle	?	?	?
strip width	0.01 cm	0.02 cm	0.03 cm
assumed resolution	0.0028 cm	0.0058 cm	0.0087 cm

Table 2:

the stereo chamber and Silicon tracker. Table 3 lists the specifications for the three alternative designs.

	Silicon	Cathode Pad	Stereo
num. layers	6	8	16
rmin:rmax	5.0:15.5	5.5:22.5	5.5:23.5
num. cells per layer	3000	64 - 156	64 - 156
assumed resolution	0.0028 - 0.0087 cm	0.02 cm	0.02 cm
total thickness (r.l.)	0.02	0.02	0.005

Table 3:
q

2.3.1 Cathode Pad Chamber

The cathode pad chamber is a cylindrical wire chamber with all wires running axially; with adjacent wire planes separated by cylindrical, metallized cathode planes. To efficiently collect the ionization charge from a traversing track, the wire planes consist of alternating sense wires and field wires. The sense wire voltage is positive, the field wires' negative, while the cathode planes are held at ground potential. The cathode plane is segmented into rectangular pads so that the image charge induced on the cathode plane by a track's arriving "avalanche" can be digitized and the mean of the distribution determined to yield the z-position of the track avalanche along the axial wire. Thus, we read out the time from the anode wire to get a precise r-phi measurement point and the centroid of the induced cathode pad charge distribution to get the r-z position of the track. Table cathode_pad_specs lists the specifications for the cathode chamber design.

2.3.2 Stereo Chamber

The central tracker must fit within the super-conducting solenoid magnet and the associated central calorimeter and time-of-flight counters. It must also not obstruct forward tracks (35 deg.). The resulting volume is a cylindrical shell with inner radius of 5 cm and outer radius of 22 cm, with conical endplates. The inner and outer cylindrical walls form the gas enclosure and provide the compressional force to offset the wire tension load of about 175 Kg. The conical endplates must precisely fix the endpoints of the wires as well as hold the high-voltage and signal distribution networks. A conceptual layout is shown in Figs. 1, showing a side-view and in Fig. 2 a view of a few wires in two superlayers, showing the stereo angle.

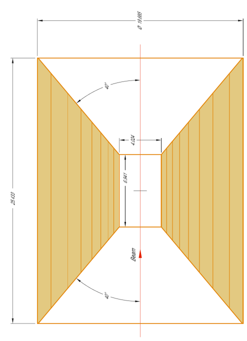

Figure 1: Resolution plotted versus particle momentum for 30 deg. tracks. Subfigures a, b, c and d show the momentum, theta, phi and vertex resolutions, respectively. Three options are shown: solid- 3 SVT planes + CC + 3 DC planes; dashed- CC + 3 DC planes; dotted - 3 DC planes

2.3.3 Cell Design

There are a total of eight super-layers with two layers each. The eight superlayers have 64, 78, 90, 104, 116, 130, 142 and 156 drift cells per layer, respectively for a total of 1760 instrumented anode wires with the drift distance varying from 0.26 to 0.42 cm. The two layers within a superlayer will have their wires arranged in a half-cell-staggered hexagonal configuration achieved by layering two field wire planes followed by an anode wire plane, then two more field wire planes, another anode plane, etc. Fig. 3 shows the cell structure as viewed from the conical endplate.

The anode wires' times will be read out to provide an r, ϕ measurement of the track by converting the drift time into a drift distance. By comparing the apparent r, ϕ point from adjacent superlayers which have a different stereo angle, we will be able to infer the z-position to an accuracy which is approximately larger than the r, ϕ resolution by a factor $1/tan\theta$.

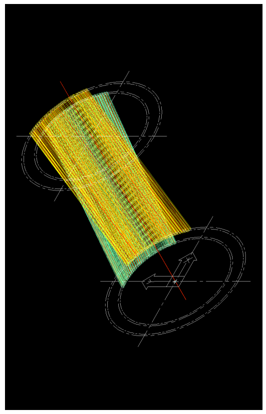

Figure 2: Resolution plotted versus particle momentum for 30 deg. tracks. Subfigures a, b, c and d show the momentum, theta, phi and vertex resolutions, respectively. Three options are shown: solid- 3 SVT planes + CC + 3 DC planes; dashed- CC + 3 DC planes; dotted - 3 DC planes

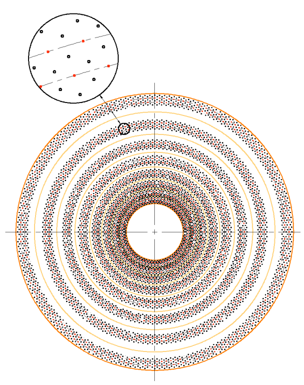

Figure 3: Resolution plotted versus particle momentum for 30 deg. tracks. Subfigures a, b, c and d show the momentum, theta, phi and vertex resolutions, respectively. Three options are shown: solid- 3 SVT planes + CC + 3 DC planes; dashed- CC + 3 DC planes; dotted - 3 DC planes

2.3.4 Central Silicon Tracker

The central Silicon tracker design consists of three double-sided Silicon strip detectors. Each detector plane is formed as an hexagonal shell with the Silicon strips running in approximately the z-direction. This detector has good intrinsic resolution in the r-phi coordinate. It relies on a small stereo angle to determine the r-z position of tracks. To avoid dead areas, the hexagonal shells formed by the different layers are not perfectly parallel to z, but have a slight conical opening toward the back (upstream) side. Both the conical opening angle and the allowed stereo angle of the strips is equal to 1.5 degrees. Table central_silicon_specs lists the specfications for the central Silicon tracker.

3 Rate Considerations

Using a modified version of the EGS program, we simulated the total hadronic and electromagnetic particle fluxes generated when an electron beam is incident upon a liguid Hydrogen target with a luminosity of 10ˆ35. We calculated the total flux through a measurement layer during its active (measurement) time and multiplied by the probablility of the particle interacting in that layer and divided by the number of cells in the layer to get an estimate of the fractional occupancy of that layer due to background. Our experience with the present CLAS detector is that track-finding is higly efficience if the accidental occupancy is less than 5% using our present algorithms. In Table rate_effects we show the number of cells, the detector live-time, the flux per layer, the interacting flux per layer, and finally the expected accidental occupancy per layer for a luminosity of 10ˆ35 and for our "standard" solenoidal Moller shield.

4 Single-track Resolution

4.1 MOMRES (program to simulate resolution)

The MOMRES program was written by Bernhard Mecking. It calculates a particle trajectory as a straight line until it reaches an area of non-zero magnetic field at which point it approximates the trajectory as a series of circular arcs with radius given by the Lorentz force. This "perfect" trajectory is then smeared by multiple-scattering and measurement error effects. At each potential scattering plane a multiple scattering angle is randomly calculated with magnitude given by the radiation length and thickness of the material in question. This deviation from the ideal trajectory is then followed to the next plane with material thickness present and a new scattering angle is calculated and this vector followed until the next material plane, as so on. In this way a sequence of points corresponding to an ideal trajectory which has undergone random multiple scattering is generated. Each of the points at a specified measurement plane is then randomly scattered according to a Gaussian distribution with a width given by the assumed measurement accuracy of the detector plane in question. The resulting points form an approximate "real" measured trajectory. This trajectory is then fit to the ideal shape, adjusting the starting point, angle and momentum of the ideal trajectory form. Doing this many times yields a distribution in momentum, starting position and angle and thus an estimate of the resoltuion in each of these variables.

The input to MOMRES is thus a table of material and measurement planes characterized by their position (path length), thickness, radiation length and, in the case of an active measurement plane, the expected position resolution of the plane. Two additional inputs to the program are a file containing the value of the B-field as a function of path length and a table of momentum which the program loops over. The output is an estimate of the resolution in momentum, starting position and angle due to the two effects: multiple scattering and measurement error. The source code for MOMRES is kept under cvs in cvs/12gev/momres.

4.2 Input files (material and plane resolution for different options)

We used MOMRES to study various detector options. Each option is specified by a separate MOMRES input file. Table momres_option_files gives a brief description of the different options we studied and the name of the MOMRES input file which is kept under cvs in cvs/12gev/momres.

4.3 Results (momentum, angle and position resolution)

We studied the position, angle and momentum resolution for a number of possible detector options using MOMRES. Our procedure was to produce a MOMRES input file which characterized the detector position, material thickness and estimated hit resolution for a particular track angle. We also produced a B-field file which was a tabulation of the B-field strength versus path length for a particular track angle. These, and the desired range of momenta, was the input to MOMRES. As stated in the previous section, MOMRES calculated the expected components of the resolutions due to multiple scattering and mesurement resolution, respectively. We fit these outputs to the expected kinematic form (see formulas dp/p, dtheta and dx for the kinematic dependence). From these fits we extracted two parameters (sig1 and sig2) for each of the three terms (dp/p, dx, dtheta). These six parameters abstract the output of MOMRES. In addition, we calculated the angle resolution in the non-bend plane in a manner analagous to that of MOMRES, using estimators for the effects of multiple scattering and measurement error and fitting the resulting smeared trajectory by a straight line with adjusted starting position and angle and extracting the sig1 and sig2 parameters which characterize the resolution in this out-of-bend-plane angle. Thus, eight parameters for each value of track angle fully characterize the tracking resolution for any one detector option. Figure 4 shows the momentum, theta, phi and vertex resolutions for three detector options for tracks emitted at 30 degrees.

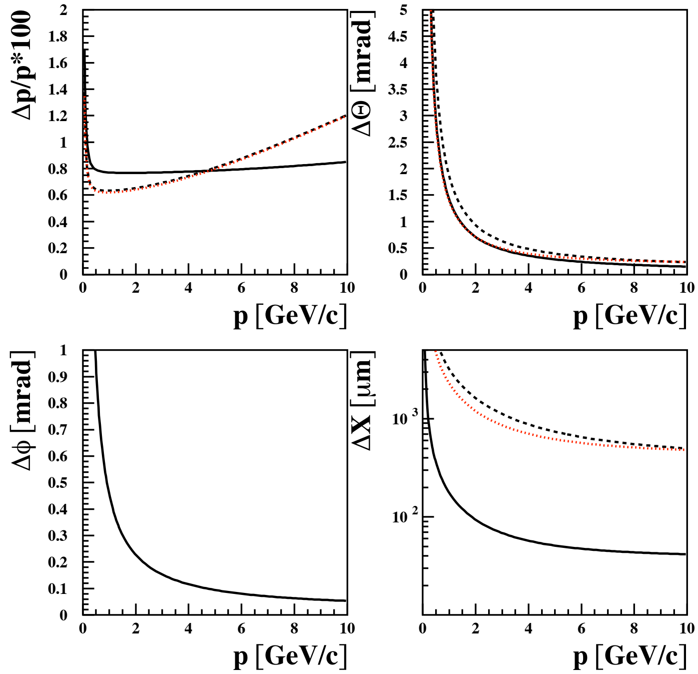

Figure 4: Resolution plotted versus particle momentum for 30 deg. tracks. Subfigures a, b, c and d show the momentum, theta, phi and vertex resolutions, respectively. Three options are shown: solid- 3 SVT planes + CC + 3 DC planes; dashed- CC + 3 DC planes; dotted - 3 DC planes

Figure 5 shows the momentum, theta, phi and vertex resolutions for three detector options for tracks emitted at 90 degrees; i.e. into the central detector.

5 Event Acceptance and Resolution

We use a series of programs to calculate the acceptance and reconstructed physics parameters for event types of interest. An event generator, clasev, loops over events of choice and, within a particular event, over the associated outgoing hadrons. Clasev calls fastmc to determine if a particular track is accepted and to obtain the final values for its 4-momentum after smearing by the expected resolution due to multiple scattering and measurement error. Physics quantities of interest, for example, missing-mass distributions, can then be generated from the accepted and smeared hadronic candidates.

5.1 clasev (event generator)

The program clasev serves as an event generator and analysis program. Depending on the value of input flags, it generates certain types of events; that is, it produces a set of 4-momenta for the primary hadrons in the hadronic center-of-mass and allows some of them to decay into the final-state hadrons and transforms their momenta to the lab system. For each final-state track, it calls fastmc to determine if the track falls within a fiducial acceptance window and to determine its final, smeared lab momentum. It then produces selected physics analysis variables such as missing-mass from calculations involving the

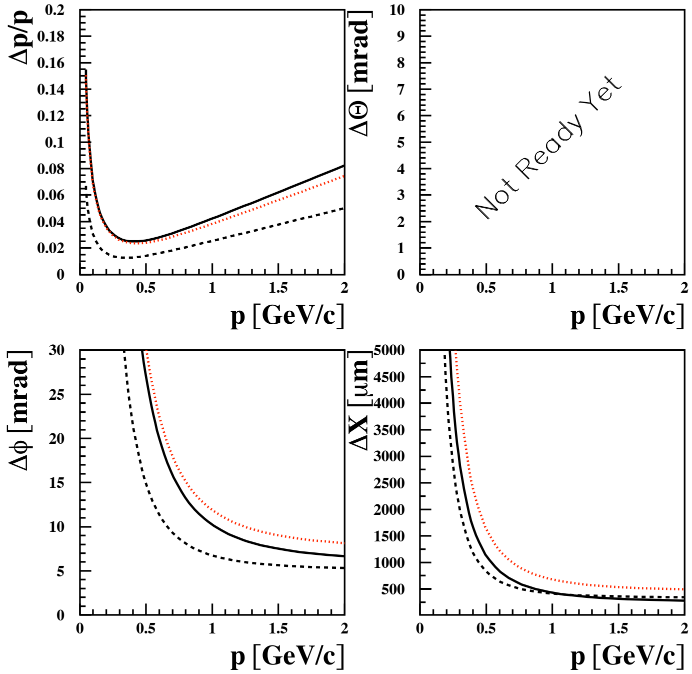

Figure 5: Resolution plotted versus particle momentum for 90 deg tracks. Subfigures a, b, c and d show the momentum, theta, phi and vertex resolutions, respectively. Three options are shown: solid- 3 SVT planes; dashed- 16 DC-stereo planes; dotted - 8 DC-cathode pad planes

smeared momenta of those tracks which were accepted. The program clasev is kept under cvs in cvs/12gev/fastmc/clasev.

5.2 fastmc (program to parameterize single-track acceptance and resolution)

The program fastmc is used to simulate the physics performance of the CLAS12 detector. The fastmc routine takes as input the particular option chosen (set of detectors and B-field setting) and from that option chooses a table of fiducial cuts which deine the acceptance for a particle based on whether it's in- or out-bending as a function of its momentum and angles and also chooses a table of parameters which defines the momentum and angular resolution as a function of momentum and angle. The program fastmc as well as the input files appropriate to different detector options are kept under cvs in cvs/12gev/fastmc.

5.3 Results (missing-mass resolutions for CLAS12)

Figure **??** shows the missing mass expected for the CLAS12 detector for these kinds of events —-

Figure 6: Missing mass recoiling from —-

6 Estimated Costs

7 Conclusions

7.1 Forward tracking conclusions

The forward tracking system, as designed, should be able to achieve the design momentum, angle and position resolutions required for the CLAS12 physics program in a background environment expected at a luminosity of 10ˆ35. For completeness, we show two options: with and without the forward Silicon strip tracker. The momentum and angle resolutions are similar for the two options. The option with the forward Silicon vertex detector naturally gives much better vertex resolution.

7.2 Central tracking conclusions

The options considered all achieve a momentum and angle resolution which is well-matched to the expected resolution from the forward tracking system.

The cathode pad option has approximately the same momentum and angle resolution as the stereo chamber option and has a rate capability about 2.5 times better. However, its successful operation depends on a low electronic noise environment and so this option is riskier. It is also substantially more costly than the stereo chamber option.

We designed the Silicon option to give roughly the same resolution as the gas chamber options by limiting its radius (the resolution improves as rˆ2). The channel count and estimated cost are much higher than the stereo chamber option, however its rate capability is much higher.

The stereo option achieves the resolution design goal and should operate at a luminosity of 10ˆ35.